Biological Journal of the Linnean Society, 2021, **133**, 1110–1125. With 7 figures.

The contribution of functional traits to the understanding of palaeoenvironmental changes

LÉA TERRAY[1,*], EMMANUELLE STOETZEL[2], ANTHONY HERREL[3] and RAPHAËL CORNETTE[1]

[1]*Institut de Systématique, Evolution, Biodiversité (ISYEB), Muséum National d'Histoire Naturelle, CNRS, Sorbonne Université, École Pratique des Hautes Études, Université des Antilles, CP50, 57 rue Cuvier, 75005 Paris, France*
[2]*Histoire naturelle de l'Homme préhistorique (HNHP), Musée de l'Homme, Muséum national d'Histoire naturelle, CNRS, Sorbonne Université, Palais de Chaillot, 17 place du Trocadéro, 75016 Paris, France*
[3]*Mécanismes Adaptatifs et Evolution (MECADEV), Muséum National d'Histoire Naturelle, CNRS, 55 rue Buffon, 75005 Paris, France*

Received 26 January 2021; revised 15 March 2021; accepted for publication 16 March 2021

Performance traits implicated in feeding interact directly with the environment and are consequently relevant ecological indicators. However, they have rarely been used to better understand palaeoenvironmental variation. Here, we evaluate the usefulness of a performance (i.e. functional) trait, estimated bite force, in reconstructing the palaeoecology of shrews. We investigate the relationships between mandible morphology, bite force estimates and the ecological context. We use geometric morphometrics to quantify mandible shape diversity in shrews of the archaeological site El Harhoura 2 (Rabat, Morocco), dated from the Late Pleistocene to the Holocene. Morphological groups were used instead of taxa as units of diversity. To explore how phenotypic traits are linked to their environment, they were compared with palaeoenvironmental inferences for the El Harhoura 2 site extracted from the literature. Morphological groups acted as phenotypic response units. Estimated bite force was related to palaeoenvironmental variation over the considered period, with a particular sensibility to arid/humid transitions. The complementarity of morphological and performance indicators allowed us to infer functional convergence and divergence among shrews. Our results suggest that functional traits may be relevant indicators of changes in palaeoenvironments. This approach opens up new possibilities to explore the impact of environmental changes on extinct organisms.

ADDITIONAL KEYWORDS: bite force – functional traits – geometric morphometrics – modularity – palaeoenvironments – shrews.

INTRODUCTION

Performance traits provide a direct link between ecology, morphology and fitness (Arnold, 1983; Wainwright, 1994). They reflect the ability of individuals to perform ecologically relevant tasks (Irschick *et al.*, 2008) and are subject to selection (Irschick *et al.*, 2008). In animals, performance traits are dependent on skeletal structures, variation in muscular anatomy, contractile physiology and variation in biomechanical traits such as lever arms. Consequently, the relationship between morphological and functional traits is complex (Wainwright, 1994; Irschick *et al.*, 2008). Different morphological traits can generate similar functional outputs by redundancy (Alfaro *et al.*, 2005), which may lead to functional convergence in organisms living in environments requiring similar performance abilities (Wainwright, 2005; Young *et al.*, 2007, 2010). Conversely, one morphological trait can affect different performance traits through trade-offs and facilitation. Trade-offs occur when there is a conflicting demand on a phenotypic trait through its differential implication in several performance traits (Garland & Losos, 1994; Van Damme *et al.*, 2003; Walker, 2007, 2010; Langerhans, 2009; Holzman *et al.*, 2011; Vanhooydonck *et al.*, 2011).

*Corresponding author. E-mail: lea.terray@mnhn.fr

Facilitation, on the other hand, occurs when a similar demand is exerted on a phenotypic trait by several different performance traits (Walker, 2007). Therefore, a complex "many-to-many" morphology-performance relationship may exist (Bergmann & McElroy, 2014), implying that morphological and functional traits may not respond similarly to changes in the environment. Thus, functional traits may be relevant candidates to function as ecological indicators, complementary to morphological traits.

Feeding is the function related to dietary ecology (Schwenk, 2000). Bite force is a performance trait implicated in feeding. It is a performance trait directly linked to diet through the mechanical demands imposed by variation in the mechanical properties of food items (Anderson *et al.*, 2008; Herrel *et al.*, 2008; Dumont *et al.*, 2009; Santana *et al.*, 2010; Maestri *et al.*, 2016). Changes in diet associated with bite force are considered one of the main drivers of diversification in mammals (Christiansen & Wroe, 2007; Monteiro & Nogueira, 2011). Thus, bite forces may be a powerful ecological proxy and have been widely used to characterize dietary ecology in vertebrates (e.g. Freeman, 1979; Losos, 1992; Herrel *et al.*, 2002; Huber, 2005; Kerr *et al.*, 2017).

Studies on bite force in fossil taxa are common as they may provide insights into the behavioural ecology of extinct taxa (e.g. Erickson *et al.*, 1996; Therrien, 2005; Wroe *et al.*, 2005; Lappin *et al.*, 2017; Rinderknecht *et al.*, 2019). However, to our knowledge, estimates of bite force have only rarely been applied to better understand palaeoenvironmental variation. Commonly, such inferences rely on community compositions and/or the characterization of particular morphotypes (e.g. (Fernandez-Jalvo *et al.*, 1998; Stoetzel *et al.*, 2011; Comay *et al.*, 2019; Royer *et al.*, 2020; López-García *et al.*, 2021). These approaches associate a particular biological feature to a specific environment. However, an organism's dietary ecology can be more accurately inferred from bite force than by categorical ecological classifications (Santana *et al.*, 2010). Thus, bite force has a strong potential to contribute meaningfully to the understanding of palaeoenvironmental variation.

Functional aspects are also important determinants of morphological integration. This concept defines the covariation patterns that exist between morphological traits (Badyaev & Foresman, 2000, 2004; Young & Badyaev, 2006; Klingenberg, 2008; Klingenberg & Marugán-Lobón, 2013). As a result of selection on performance, traits implicated in a same function interact strongly, making them vary together (Klingenberg, 2008). This may be particularly the case when they are linked through muscle insertions providing physical and mechanical links between structures (Cheverud *et al.*, 1997; Mezey *et al.*, 2000; Klingenberg *et al.*, 2003; Klingenberg, 2004). Thus, changes in the strength of integration in the feeding apparatus could be related to changes in bite force. Moreover, the less the modules in a structure like the mandible covary together (i.e. the more modular they are), the more disparate are the organisms that can be produced (Goswami *et al.*, 2014). Modularity patterns may consequently also be related to bite force disparity. Moreover, changes in modularity are known to respond to environmental stresses (Badyaev & Foresman, 2000). In the light of these facts, modularity in the feeding apparatus may also be a relevant indicator for understanding variation in palaeoenvironments.

The Moroccan archaeological site El Harhoura 2 (EH2) is located in the Rabat-Témara region, on the North Atlantic coast of Morocco. It is divided into 11 archaeo-stratigraphical levels covering a time period from the Late Pleistocene to the Holocene. Phenotypic evolution related to environmental variation has been extensively studied at this site (Stoetzel, 2009, 2017; Stoetzel *et al.*, 2010, 2011, 2012b, 2013, 2017). Small mammals such as rodents and shrews are a relevant model to consider palaeoenvironmental variation (e.g. Valenzuela *et al.*, 2009; McGuire, 2010; Escudé *et al.*, 2013; Verde Arregoitia *et al.*, 2017). The biogeographical and ecological characteristics of species (such as diet, habitat and soil), as well as the global composition of the small vertebrate communities in the different studied levels, allowed palaeoenvironmental inferences at EH2 (e.g. Stoetzel *et al.*, 2011, 2013, 2017). Among the remains recovered at EH2, shrew mandibles have been given peculiar attention (Cornette *et al.*, 2015a, c). Mandible shape is known for being highly plastic and often varies with environmental conditions in these animals (Badyaev & Foresman, 2000; Caumul & Polly, 2005; Cornette *et al.*, 2015a, c; Souquet *et al.*, 2019).

In the present study, we sought to understand the relationship between the morphology of the mandible in shrews, its modularity and the estimated bite force over time. We further explored whether a functional trait (bite force) can provide relevant information for the understanding of palaeoenvironments. Our approach is divided in three steps. (1) To evaluate global morphological diversity, shrews were divided into morphological groups (MGs). This characterization of biodiversity was chosen instead of species. MGs allow for the consideration of variation at several levels of diversity (inter- and intra-specific), which makes it a relevant approach to characterize environment-related selection which acts at both levels (Erwin, 2000; Lande, 2009; Boutin & Lane, 2014; Hautmann, 2020). We expected identified MGs to be functional response units to changes in the environment, as has been suggested in previous studies (Read *et al.*, 2014; Khare *et al.*, 2017). (2) Bite force was estimated through

the mechanical potential. Because performance and morphology are not strictly related, selection can apply differently at both levels of organization (Irschick *et al.*, 2008). Thus, quantifying variation in the mechanical potential may allow us to detect selection events undetectable through morphological proxies. (3) Finally, variation in modularity was characterized. An increase in modularity in shrew mandibles may allow morphological diversification within a population utilizing the same resources irrespective of selection on function (Young *et al.*, 2007, 2010) and as such be associated with variation in the environment.

MATERIAL AND METHODS

EL HARHOURA 2 CAVE AND DATA COLLECTION

El Harhoura 2 cave (33°57'08.9" N / 6°55'32.5" W) is an archaeological site located on the Moroccan Atlantic coast, a few kilometres south of Rabat. The cave was occupied by Middle Stone Age, Later Stone Age and Neolithic human populations and has yielded numerous archaeological materials as well as the remains of large and small vertebrates (Nespoulet *et al.*, 2008; El Hajraoui *et al.*, 2012; Stoetzel *et al.*, 2014). From top to bottom, the stratigraphy of EH2 cave is structured in 11 layers. Eight of these levels are well dated and were included in this study (L1, L2, L3, L4a, L5, L6, L7, L8) (Jacobs & Roberts, 2012; Jacobs *et al.*, 2012; Janati-Idrissi *et al.*, 2012; Ben Arous *et al.*, 2020a, b). Palaeoenvironmental data were deduced from faunal communities (Stoetzel, 2009; Stoetzel *et al.*, 2011, 2012a, b, 2014). An alternation of humid and arid periods has been documented and the landscape was mainly dominated by steppes with an increase in more wooded areas and water ponds during humid periods (Fig. 1).

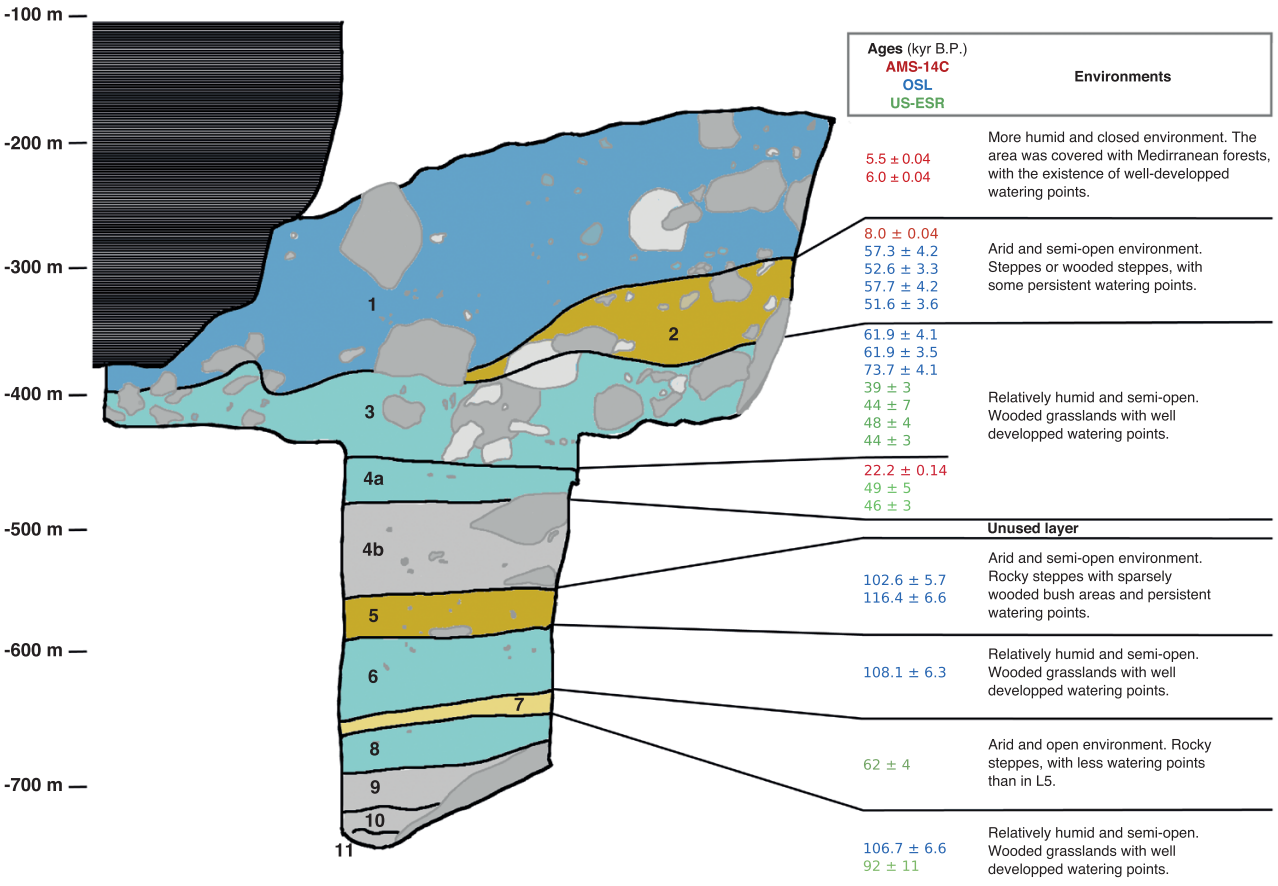

Figure 1. Stratigraphy, datation and characteristic environments of the eight layers of EH2 used in this study (Stoetzel, 2009; Jacobs *et al.*, 2012; Janati-Idrissi *et al.*, 2012; Nespoulet & El Hajraoui, 2012 - excavation report; Stoetzel *et al.*, 2012a; Ben Arous *et al.*, 2020a, b). Three datation methods were used: AMS-14C (based on organic remains), US-ESR (Combined Uranium Series and Electron Spin Resonance) and OSL (Optical Stimulated Luminescence). Light blue layers: humid and open environment; dark blue layers: humid and close environment; light yellow layers: arid and open environment; dark yellow layers: arid and semi-open environment. Layers unused in this study are in grey.

The material studied here is temporarily housed at the Muséum National d'Histoire Naturelle, Paris, France. It was sampled during the 2005–2009 excavation campaigns of the El Harhoura-Témara Archaeological Team (directors R. Nespoulet and M.A. El Hajraoui). Four species of white-toothed shrews are represented: the material is largely dominated by *Crocidura russula* but *Crocidura lusitania*, *Crocidura tarfayensis* and *Crocidura whitakeri* were also present (Cornette *et al.*, 2015a, c). Among archaeological remains complete mandibles are rare and most of the material is fragmented. Nevertheless, mandible fragments also carry relevant morphological and palaeoenvironmental information (Cornette *et al.*, 2015a, c) and can be used to increase the sample. Here we used complete mandibles (Clpt) and three types of mandible fragments (A, B, C). Chosen fragments are those whose shape best enables species to be distinguished (Cornette *et al.*, 2015a). Fragmentation patterns are illustrated in Figure 2. Extant material (Act) from the Rabat area was added to extend the timeline to present day (*C. lusitania* and *C. tarfayensis* are no longer present in the area). The number of complete and fragmented mandibles studied is indicated in Table 1. Data acquisition is described in Cornette *et al.* (2015a).

Geometric morphometrics

Two dimensional geometric morphometric analyses were used. All mandibles could not be analysed together because remains from various fragmentation patterns were not directly comparable. We performed separate shape analyses for each fragment type (Cplt, A, B and C) following the same protocol. Mandibles were analysed through a landmark- and sliding semi-landmark-based approach allowing the description of the shape of biological relevant areas without anatomical landmarks (Bookstein, 1996; Zelditch, 2004; Gunz *et al.*, 2005; Cornette *et al.*, 2013). Landmark locations for each fragment type are indicated in Figure 2. Semi-landmarks were slid to minimize the bending energy. Generalized Procrustes Analyses (GPA) were performed on each data set (Cplt, A, B and C) to make objects comparable by removing effects of translation, rotation and scale (Rohlf & Slice, 1990). Resulting shape coordinates are the Procrustes residuals. These two last steps were performed using the "gpagen" function of the "geomorph" package (Adams & Otárola-Castillo, 2013) in R Core Team (2020). To reduce data dimensionality, principal component analyses were performed on Procrustes residuals for each data set (Cplt, A, B and C) and we retained 95% of shape variation for the following analyses (Baylac & Frieß, 2005). All analyses were performed using R Core Team (2020).

Morphological groups

To assess shape diversity, mandibles were partitioned into morphological groups. First, complete mandibles (Clpt) were clustered based on their shape. To do so a morphological K-nearest neighbour method (KNN) was used. This method is adapted to small data sets,

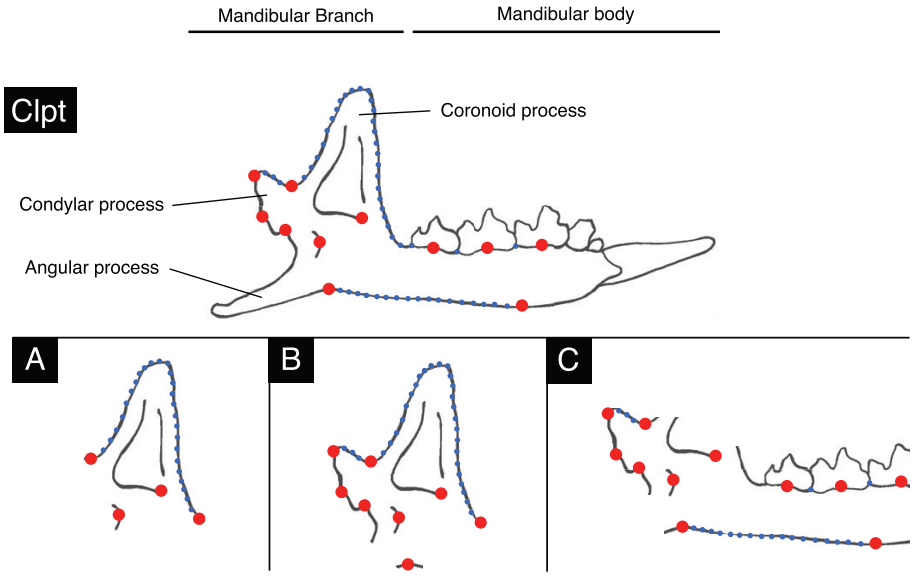

Figure 2. Types of fragments and their landmark (red points) and semi-landmark (blue points) locations. Clpt: complete mandibles; A: fragmented mandibles of type A; B: fragmented mandibles of type B; C: fragmented mandibles of type C.

as is the case here, because it is a non-parametric classification. In this algorithm, each shape object is assigned to its nearest neighbour cluster. The "clues" function of the "clues" package (Wang *et al.*, 2007) proposes an unsupervised KNN, meaning that the number of clusters is inferred from the data itself, favouring the most robust partitioning of the data set. The robustness of the clusters is assessed by the Silhouette index (SI) (Kaufman & Rousseeuw, 1990) which measures the strength of the clusters. SI is comprised between -1 and 1. The more SI is close to 1 (i.e. SI > 0), the more data points are correctly assigned to their clusters, and conversely the more SI is close to -11 (i.e. SI < 0), the more data points are misassigned (Wang *et al.*, 2007).

To visualize the morphological groups identified, the morphospace of complete mandibles (Cplt) was plotted using the three first axes of the principal component analysis computed on the Cplt data set. Deformations along axes were computed using the function "PlotRefToTarget" from the "geomorph" package (Adams & Otárola-Castillo, 2013). Thin-plate spline deformation grids representing differences between the extreme shapes of each axis and the global mean shape of Cplt mandibles were generated.

Next, we tested the robustness of the morphological groups identified on complete mandibles (Clpt) for each fragmentation pattern. Artificial A, B and C fragments were computed from complete mandibles (Clpt) and strengths of the clusters based on fragments were assessed using SI. This was achieved using the "get_Silhouette" function of the "clues" package (Wang *et al.*, 2007).

Finally, the belonging of true A, B and C mandible fragments to the morphological groups was determined a posteriori using the KNN classification algorithm with the "knn" function of the "class" package (Venables & Ripley, 2002). Mean shapes of each morphological group were computed from complete mandibles (Clpt) using the functions "mshape" and "warpRefOutline" of the "geomorph" package (Adams & Otárola-Castillo, 2013).

Table 1. Abundance of remains studied (Clpt: complete mandibles; A, B, C: fragmented mandibles; Act: actual mandibles; L1: mandibles of the layer 1 of EH2 [the same apply to L2, L3, L4a, L5, L6, L7, L8])

Layer	Clpt	A	B	C	TOTAL
Act	16	-	-	-	16
L1	2	1	-	2	5
L2	2	4	1	2	9
L3	3	1	1	1	6
L4a	2	1	-	1	4
L5	10	-	2	3	15
L6	10	2	4	9	25
L7	9	7	13	10	39
L8	-	6	10	11	27
TOTAL					146

Mechanical potential

The mechanical potential as used in this study is the ratio of the muscle moment arm to the jaw outlever. As such it is dependent on the geometry of the skull and mandible and the insertion of the masticatory muscles (Herrel *et al.*, 2008; Chazeau *et al.*, 2013; Manhães *et al.*, 2017; Ginot *et al.*, 2018, 2019). In particular, mandible shape is known for being a good estimator of bite force (Brassard *et al.*, 2020a, b). As a proxy for overall mechanical potential, we choose the mechanical potential of the temporalis muscle. This is one of the main muscles involved in bite force generation in shrews (Herrel *et al.*, 2008; Santana *et al.*, 2010; Brassard *et al.*, 2020a). It was estimated based on the moment arm of the temporalis, computed from the mandible shape. The biomechanical model is presented in Figure 3. It is defined as MP = A / B, where: A is the moment arm of the temporalis, B is the jaw out-lever and MP is the mechanical potential of the

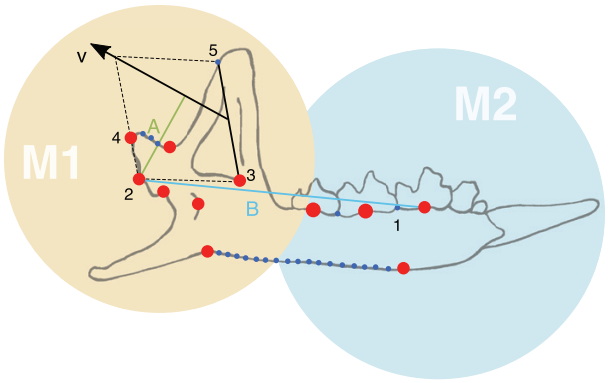

Figure 3. Biomechanical model used to estimate the mechanical potential of the temporalis muscle (MP) from mandible shape. V is the vector that starts at mid distance between landmarks 3 and 5 and has, for direction, the intersection between the line passing through landmarks 3 and 4 and the parallel of the line passing through landmarks 2 and 3 passing through 5. A is the moment arm of the temporalis (the distance between the landmark 2 and the vector). B is the jaw out-lever (the distance between landmarks 1 and 2). M1 and M2 are the definitions of the two hypothesized modules of the mandible from the literature (Cheverud *et al.*, 1997; Mezey *et al.*, 2000; Klingenberg *et al.*, 2003; Klingenberg, 2004) and landmarks implicated (C fragmentation pattern). M1: ascending ramus module; M2: alveolar region module.

temporalis. MP was computed for complete mandibles (Clpt) from Procrustes residuals.

However, MP does not reflect the phenotype in nature: because it is computed from Procrustes residuals, it does not account for size variation in the data set, nor for compensatory effects of musculature. Moreover, it only considers a single force—the temporalis muscle—which is applied uniformly (Young *et al.*, 2007). All these parameters are important drivers of the mechanical potential, in particular size (Wroe *et al.*, 2005; Freeman & Lemen, 2008; Herrel *et al.*, 2008; Chazeau *et al.*, 2013; Manhães *et al.*, 2017; Ginot *et al.*, 2018, 2019; Brassard *et al.*, 2020a). In order to increase the accuracy of our estimate of bite force, we corrected MP to take size into account.

It is known that MP is linearly correlated to mandible/skull size in some mammals, including shrews (Nogueira *et al.*, 2009; Cornette *et al.*, 2015b; Manhães *et al.*, 2017; Ginot *et al.*, 2018; Brassard *et al.*, 2020a). As MP is computed from mandible shape, this means that it has an allometric component, i.e. even if MP is size-free, a part of the MP results from the influence of size. To confirm this assumption in our data set, we tested it on complete mandibles (Cplt) by performing a regression of the log-transformed centroid size on the log-transformed MP using the "lm" function of the "stats" package. Centroid size (Csize) is a size estimator widely used in geometric morphometrics. It is defined as the square root of squared distances of all landmarks of a mandible from its centroid (Klingenberg, 2016).

Corrected MP (cMP) was subsequently expressed as: cMP = MP + f(size) **(eqn. 1)**, where MP is the mechanical potential and f(size) is the part of cMP due to size. It is also known that $\log_{10}$ bite force is linearly correlated to size (Wroe *et al.*, 2005; Chazeau *et al.*, 2013; Manhães *et al.*, 2017; Ginot *et al.*, 2019; Brassard *et al.*, 2020a). Thus, for cMP to be a good estimator of bite force, log-transformed cMP must also be linearly correlated to size. So, in **(eqn. 1)** we have f(size) = a*size + b **(eqn. 2)**. The objective here is to determine a and b.

We assume that the allometric part of MP is proportional to the influence of size on MP. Thus, a and b of **(eqn. 2)** can be found by performing a linear regression of size on MP. However, our data have a temporal component that we need to consider, otherwise we may lose part of this temporal information as MP and size are both related to time. We performed a multivariate regression of size and time on MP. Log-transformed values of MP and Csize were used. a and b of **(eqn. 2)** were defined with the parameters of this regression: a as the coefficient of log(Csize) and b as the intercept. We obtained: log(cMP) = log(MP) + a*log(Csize) + b **(eqn. 3)**.

To evaluate whether cMP is a good estimator of bite force, we assessed its reliability on a data set of simulated data:

1. One thousand bite forces and associated sizes were simulated. Values were randomly generated according to a normal distribution using the "rnorm" function of the "stats" package, with for bite forces the constraint of a mean of 0.3 and a standard deviation of 0.15, and for size a mean of 3500 and a standard deviation of 500. Those constraints aimed to generate a data set as close as possible to what is observed for the species present in our data set.
2. MP was computed using **(eqn. 3)**, where cMP was replaced by bite force values and with a and b arbitrarily fixed (to represent the "real" relation between MP, bite force and size in the simulated data set). Thirty couples of a and b were randomly generated using the "rnorm" function of the "stats" package and tested. They were computed in order to be similar to the a and b found previously. As the correlation between $\log_{10}$ bite force and size is strictly positive (Wroe *et al.*, 2005; Chazeau *et al.*, 2013; Manhães *et al.*, 2017; Ginot *et al.*, 2019; Brassard *et al.*, 2020a), a should be strictly positive and was generated with the constraint of a mean of 3 and a standard deviation of 3. b was generated with the constraint of a mean of 0 and a standard deviation of 5 to test positive and negative values. Tested couples of a and b are presented in Supporting Information (Table S1). To simulate measurement error, Gaussian noise was added to computed MP (error tested at 0.01, 0.05 and 0.1).
3. cMPs were calculated using **(eqn. 3)**, with a and b found previously.
4. For each pair of values in the simulated data set, we tested whether the relation between the bite force of individuals was respected by cMPs (for example, if we have two individuals X and Y such that: bite force X > bite force Y, we must also have cMP X > cMP Y). Thus, variation in cMP reflects, in a relative way, variation in bite force. Mean, minimum and maximum scores of reliability among the 30 a and b couples were computed for the three measurement error estimates.

To obtain the cMPs of fragmented mandibles (A, B and C) we predicted it from the cMPs of complete ones (Clpt) according to the following protocol. First, to evaluate the reliability of the prediction, we performed covariation analyses between artificial fragments generated from the complete mandibles (Clpt) corresponding to fragmentation patterns (A, B and C) and cMP. We used two-block partial least squares analyses (PLS) which assesses the covariance between two sets of variables. This step was done using the "two.b.pls" function of the "geomorph" package (Adams & Otárola-Castillo, 2013), which performs a PLS

adapted to shape data. Then, the cMPs of fragmented mandibles were predicted using the "plsr" function of the "pls" package (Mevik & Wehrens, 2007). This function allows prediction based on the covariation between the two variables.

Shapes associated with the strongest and weakest cMPs were computed. Those shapes were estimated based on the linear regression of cMP on shapes of complete mandibles (Cplt) using "procD.lm" of the "geomorph" package (Adams & Otárola-Castillo, 2013). They were then computed with the "warpRefOutline" function of the same package.

Changes of cMP through time were investigated in two ways:

1. Global cMP per layer. Differences between layers were tested through pairwise comparisons testing using the "pairwise.t.test" function of the "stats" package which correct for multiple testing.
2. cMP per morphological group per layer.

For both, standard deviation was computed on each layer as a measure of variance.

MODULARITY

As the abundance of complete mandibles (Clpt) per layer was not sufficient, the modularity analysis was performed based on the C fragmentation pattern on complete (Clpt) and C fragments. We divided the mandible into two modules a priori according to the hypothesized primary developmental modules defined in the literature (Cheverud *et al.*, 1997; Mezey *et al.*, 2000; Klingenberg *et al.*, 2003; Klingenberg, 2004) (Fig. 3).

To quantify the modular structure of the mandible, we computed the Covariance Ratio (CR) per layer. CR compares the global covariation between hypothesized modules relatively to the covariation within those modules (Adams, 2016). The modularity hypothesis (independence of the hypothesized modules) is verified when CR < 1. This measure is unaffected by sample size or the number of variables (Adams, 2016). It was performed using the "modularity.test" function of the "geomorph" package (Adams & Otárola-Castillo, 2013).

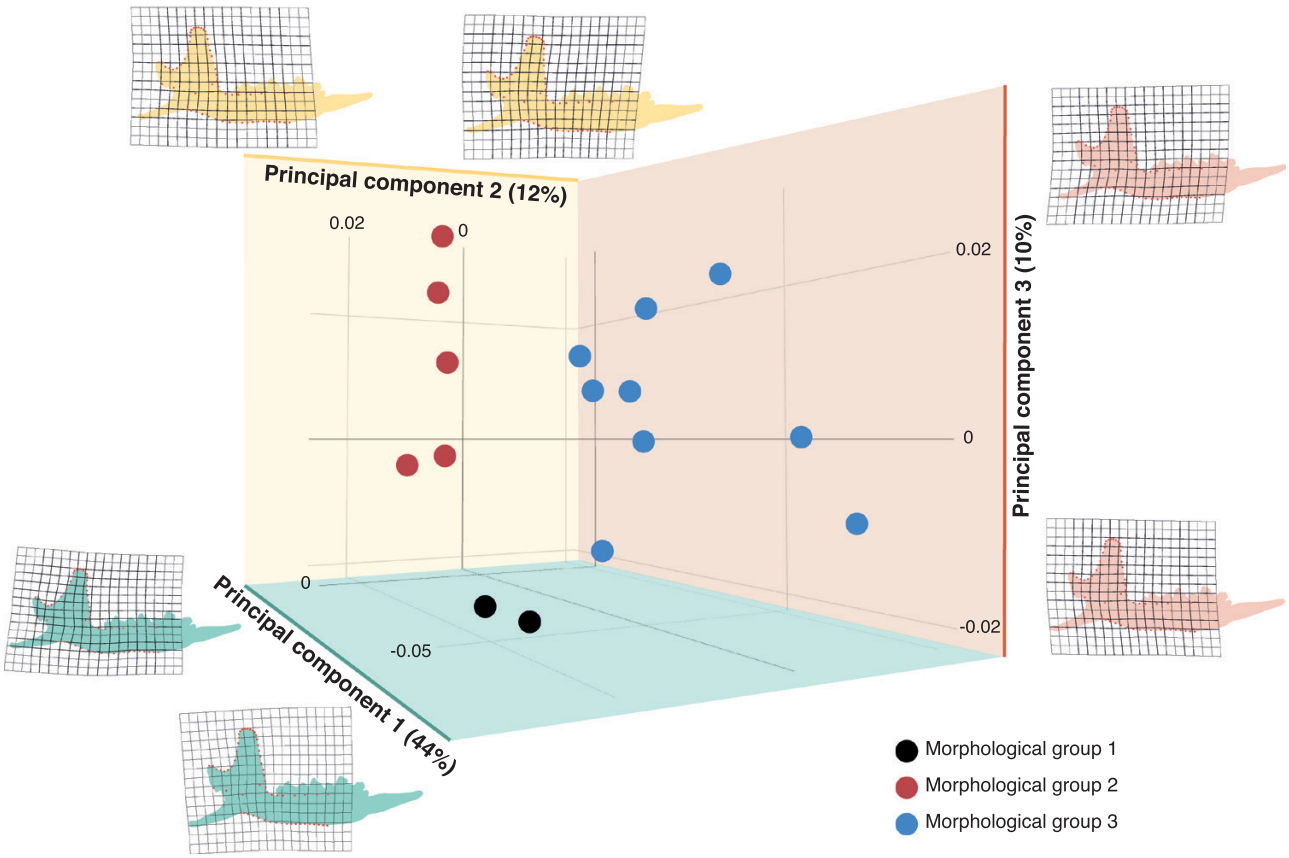

Figure 4. Principal component analysis on complete mandibles (Cplt).

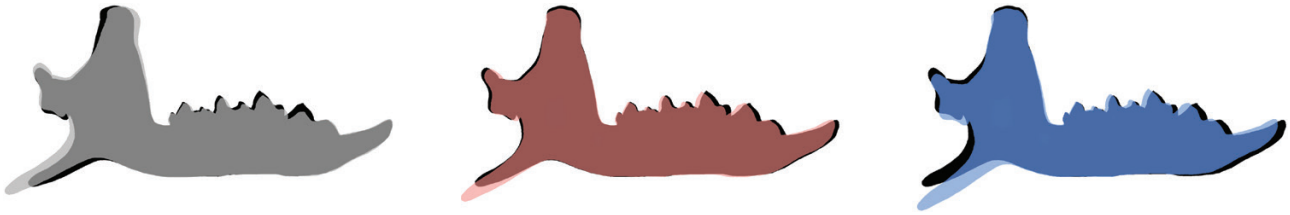

Figure 5. Mean shapes of the three morphological groups (in grey, red and blue) compared to the global mean shape (in black) of complete mandibles (Clpt).

Data availability

The data underlying this article will be shared on reasonable request to the corresponding author.

RESULTS

Morphological groups

Three morphological groups were detected among complete mandibles (Clpt). We obtained an SI = 0.15, meaning that the morphological partitions obtained with the clustering are correct. This partitioning was also valid for A, B, and C fragments (A fragments: SI = 0.1; B fragments: SI = 0.09; C fragments: SI = 0.1).

A visualization of the morphological groups on the principal component analysis of complete mandibles (Cplt) and their deformations along major axes is presented in Figure 4. Mean shapes of the morphological groups are presented in Figure 5. The first group (illustrated in grey in Fig. 5) has an elongated mandibular body, a more anteriorly inclined coronoid and a more dorsally oriented condylar process compared to the average mandible shape. The second group (illustrated in red in Fig. 5) displays a shape similar to the mean shape. The third group (illustrated in blue in Fig. 5) has a short mandibular body, a coronoid process that is slightly more posteriorly inclined and a condylar process that is more ventrally oriented.

Mechanical potential

Log-transformed MP was revealed to be weakly and negatively correlated to log-transformed Csize (R^2 = 0.014, P = 0.0029, 52 degrees of freedom). The multivariate regression **(eqn. 3)** was also significant (R^2 = 0.12, P = 0.023, 50 degrees of freedom). We obtained a = 0.30 (coefficient of log-transformed Csize) and b = -3.47 (intercept). The reliability scores of cMP based on the simulated data are indicated in Table 2.

Table 2. Reliability scores of cMP for the three tested measurement errors

Measurement error	0.01	0.05	0.10
Mean	82%	82%	81%
Max.	98%	96%	93%
Min.	66%	66%	66%

The PLS results showed that cMP is strongly related to A, B and C fragments generated from complete mandibles (Clpt) (PLS: A fragments, r-pls = 0.66, $P < 0.05$; B fragments, r-pls = 0.75, $P < 0.05$; C fragments, r-pls = 0.64, $P < 0.05$), ensuring the reliability of predicted cMPs for fragments.

Mean shapes associated with the strongest and weakest cMPs are presented in Figure 6. The shape associated with the weakest cMP (left in Fig. 6) is characterized by an elongated mandibular body and a short mandibular branch compared to the global average shape of the mandible. On the contrary, the shape associated with the strongest cMP (right in Fig. 6) displays a short mandibular body and a long mandibular branch.

Global changes in cMP through the El Harhoura 2 sequence are presented in Figure 7A. In L7, a period characterized by an open and arid environment, a great variability in cMPs co-exist compared to other layers (Fig. 7B). An important increase in average cMP is observed from L7 to L5 and then cMP decreases until present day resulting in cMP values similar to those observed in L7 (Fig. 7A). However, pairwise testing indicates that only the cMP of L5-L7 and Act-L5 are significantly different ($P < 0.05$). Raw variations of the moment arm of the temporalis (A) are also presented in Supporting Information (Fig. S2).

Changes in cMP per morphological group through time are presented in Figure 7B. Not all morphological groups show the same variation in cMP over time, nor the same degree of variability. However, the three groups display a higher variability in L7. Overall, one of the morphological groups (indicated in blue in Fig. 7B) has a higher cMP than the others. The two

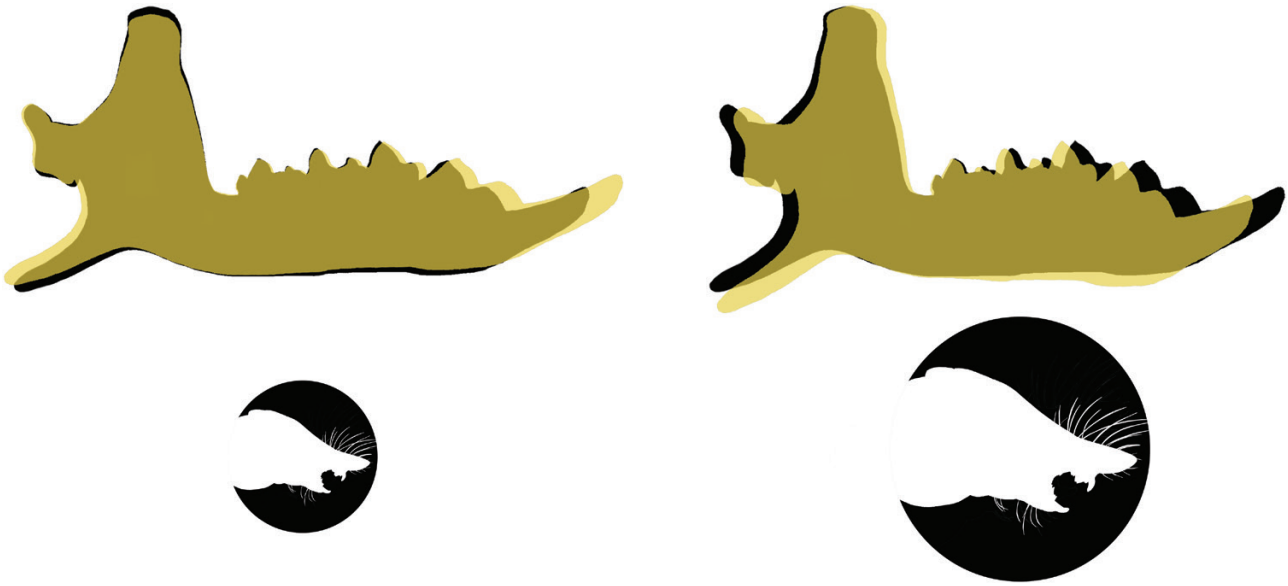

Figure 6. Mean shapes associated with the strongest (right) and weakest (left) cMP (in yellow) compared to the global mean shape (in black) of complete mandibles (Clpt). Strength of the cMPs is symbolized by the size of the shrew drawing under the models.

other groups (indicated in red and black in Fig. 7B) display similar cMP values. In L5, the cMPs of the three morphological groups converge toward high cMP values. Then, starting from L5, there is a drop in mandible shape diversity with the disappearance of one morphological group. In L4a and L3, the two remaining groups show a divergence in cMP towards respectively lower and higher values. In L2, a second diversity drop occurs with the disappearance of another group. From then onwards only one morphological group is consistently present, the two others show only few occurrences.

Modularity

Changes in CR over time are presented in Figure 7C. CR was not statistically significant in L2 and L4a. There are two main changes in CR values, first a slight increase in L7 (CR = 0.86, $P < 0.05$) followed by a strong increase from L5 to L3, with a peak in L3 (CR = 0.95, $P < 0.05$).

DISCUSSION

In this study, we aimed (1) to investigate the relationship between shrew mandible morphology, modularity and estimated biting forces (cMP) over time and (2) to evaluate whether a performance trait (bite force) could provide relevant information in the understanding of palaeoenvironments. To do so, we explored mandible shape diversity in archaeological shrews, and computed the covariation ratio and estimated mechanical potential over time. First, we discuss the meaning of morphological groups and the benefits of this approach. Next, we focus on the relation between mandible shape and mechanical potential. Finally, we address the variation in these traits over time and compare them to environmental inferences from the literature to assess their potential relevance for palaeoenvironmental studies.

Morphological groups

Over the considered period, up to three morphological groups of mandibles were found among the four shrews species present at EH2 (*C. russula*, *C. whitakeri*, *C. tarfayensis* and *C. lusitania*) (Cornette *et al.*, 2015a, c). The assessed morphological diversity is consequently above the species level. Simplification of information is a risk of the morphological group approach (Read *et al.*, 2014); however, it provides access to a partition of variability that is potentially more informative ecologically than taxonomically when the studied biological object is sensitive to environmental change (Alperin *et al.*, 2011; Read *et al.*, 2014; Khare *et al.*, 2017), which is the case for shrew mandibles (Badyaev & Foresman, 2000; Young *et al.*, 2010). The morphological groups reveal variations in the number of morphotypes independent of the number of species. For example, in the recent layers of EH2 (from L4a until L1) only one or two morphological groups are present per layer whereas all

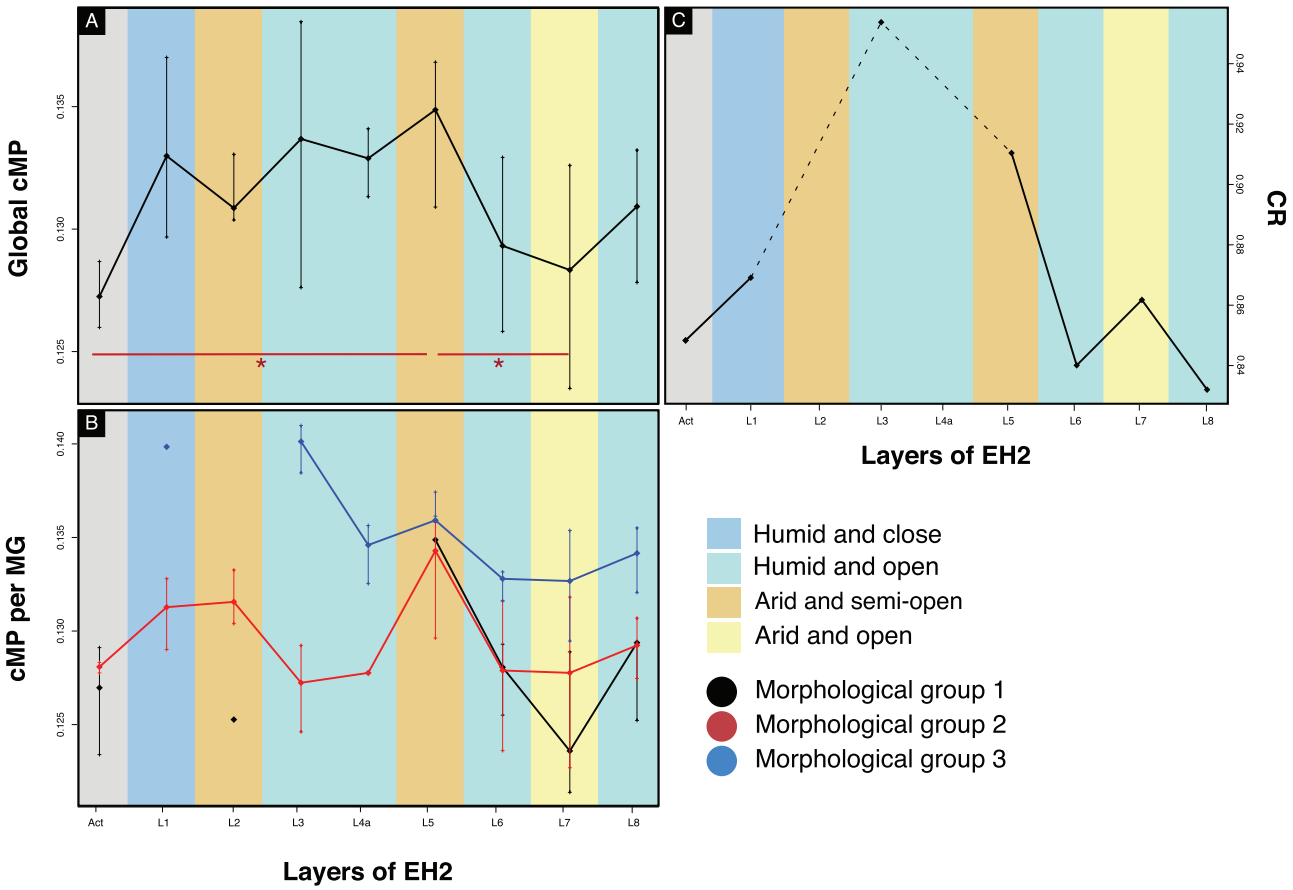

Figure 7. Global changes in cMP (A), cMP per morphological group (B) and CR (C) of the shrews of EH2, from L8 until present day (Act). Environmental conditions (Stoetzel, 2009; El Hajraoui *et al.*, 2012) are indicated by background colours. For cMP, standard deviation is indicated for each point. A: layers displaying significant different cMP (L7–L5 and L5–Act) are indicated by red asterisks. B: black is the first morphological group; red is the second morphological group; blue is the third morphological group. C: dotted lines indicate missing values.

four species are still present suggesting morphological convergence across these species (Cornette *et al.*, 2015c). The morphological groups are characterized by different functional outputs and in their response to environmental changes. Except in L5, they display a different cMP and show different trends over time, especially from L4a and L3. To sum up, morphological groups are characterized by differences in morphology, functional output and their response to environmental change. Thus, they represent morphological and functional response units to external variation.

Nevertheless, because we used only three of the five types of mandible fragments that were used in Cornette *et al.* (2015a, c), we reduced the initial sampling which can result in a potential loss of diversity. However, unused fragments were the least informative and reliable and could have introduced uncertainties into the results of this study which is why we chose to exclude them.

Mandible shape and mechanical potential

The relation between rostrum elongation and mechanical potential is intuitive as a longer rostrum increases the jaw out-lever and consequently results in a lower mechanical potential. This is illustrated by the negative correlation between MP and mandible size. This type of relation between MP and mandible size has also been observed in other mammals [e.g. Casanovas-Vilar & van Dam (2013) for squirrels, Nancy (1982) for felids]. This implies that the smallest specimens have a higher mechanical potential than the largest ones. Mechanical potential and size are both important drivers of bite force. These results suggest that the relative importance of these drivers varies between small and large specimens. Conformations may be a more important driver of bite force than size in small specimens compared to large ones. Nevertheless, the weakness of this correlation suggests that the specimens used here are rather uniform in size.

Concerning the mandibular branch, our results are consistent with Young *et al.* (2007) who found that a high mechanical potential was associated with a greater distance between the condylar and the coronoid processes. This is related to muscles of the masticatory apparatus: the coronoid process is the place of insertion of the temporalis muscle, the condylar process is the place of insertion of the external pterygoid and the angular process is the place of insertion of the internal pterygoid and the masseter. They all participate in generating bite force and impact bone shape in shrews (Furió *et al.*, 2010; Cornette *et al.*, 2015c).

The mean shapes of morphological groups display morphological features that can be related to their mechanical potential. The group displaying the highest mechanical potential (in blue on Figs 4, 5, 7) is the one with the shortest mandibular body and the closest condylar and coronoid processes, which are morphological and functional particularities related to hard diet specialists in shrews (Young *et al.*, 2007). Conversely the group with the weakest mechanical potential [in grey (Fig. 5) and in black (Figs 4, 7)] displays features characteristic of soft diet specialists in shrews (Young *et al.*, 2007). The third group [in red (Figs 4, 5, 7)] showing average features likely regroups generalist shrews. Thus, morphological groups appear to highlight ecological specializations.

Modularity might be a key concept to understand the link between morphological and functional variation. Three main decreases in modularity (i.e. increases in CR) are observed in the sequence at EH2 in L7, L5 and L3. In L7, the three morphological groups display unusual variability in cMP (it is important to note that this is the layer with the largest sample). In L5, the three morphological groups show remarkably similar cMPs, meaning similar functional outputs. Finally, in L3, the two morphological groups display highly divergent functional outputs. Each decrease in modularity (i.e. increase in CR) in the mandible is associated with an increase in the ability of a form to produce more diverse functional outputs, allowing either divergence (as in L7 and L3) or convergence (as in L5) in the cMP. These are in contradiction with Young *et al.* (2007, 2010), who found that extensive modularity allowed shrews with more diverse morphologies to produce a similar functional output. However, Young *et al.* (2010) underlined that adaptive responses are highly variable, even at a population level, which may explain the difference observed in comparison to our results. It may be the adaptive strategy here implies a different relation between mechanical potential and the modularity of the mandible. A possibility might involve variation in skull shape which was not studied here (Cornette *et al.*, 2015c).

Mechanical potential as a palaeoenvironmental indicator

When considering both global and per morphological group changes in cMP, four important functional variations were detected over time in L7, in L5, during L4a-L3 and in L2. Three of these (in L7, L5 and L2) match transitions from humid to arid environments (Stoetzel, 2009; Stoetzel *et al.*, 2011).

In L7, we observed a high morphological diversity (with the presence of the three morphological groups), the co-existence of highly diverse cMPs (Fig. 7A, B) and a decrease in modularity (Fig. 7C). An increase in the diversity in cMP could be caused by a release of selective pressures on this trait, allowing shrews with diverse abilities to survive. This could be due to the availability of more diverse resources in the environment of L7 than in those of other layers. However, the environment in L7 is characterized by an open and dry environment of arid steppes, and seems to present less ecological diversity than some other layers (Stoetzel, 2009; El Hajraoui *et al.*, 2012). Another hypothesis might be that a lack of resources drives character displacement in shrews with forms becoming highly specialized in the consumption of different resources. Moreover, the masseter and the medial pterygoid muscles also participate in generating bite force (Herrel *et al.*, 2008; Santana *et al.*, 2010; Brassard *et al.*, 2020 a, b). However, these muscles are implicated in the consumption of different types of resources, as in bats where the masseter allows the consumption of more soft resources (Santana *et al.*, 2010). Moreover, functional variation is accompanied by a decrease in modularity. Variation in the degree of covariation between mandibular modules in shrews may be related to stressful environmental conditions (Badyaev & Foresman, 2000). In the light of this fact, it is more likely that during the period covered by L7, shrews endured particularly stringent environmental conditions, with fewer and/or different available resources than before. As shrews are opportunistic, they might have switched their diet during this period inducing a release on the functioning of the temporalis muscle. However, as L7 is the layer with the largest sample this may bias our observations.

In L5, the cMPs of two morphological groups greatly increases and the cMPs of the three groups converge toward high values (Fig. 7A, B). Pairwise testing indicates that global cMP is significantly different in L5 compared to L7 and present day (Fig. 7A), and consequently supports the hypothesis of a cMP convergence towards high values in L5. This functional convergence is not associated with a convergence of the morphological groups, which is not surprising as those two types of convergence (functional and morphological) can be independent (Stayton, 2006). The group of soft

diet shrews (in black in Fig. 7B) is possibly subjected to a selection causing large-sized specimens to produce the highest mechanical potential (as illustrated in Supporting Information, Fig. S1). Here we have a case of functional redundancy: three distinct morphologies producing similar functional outputs (Alfaro *et al.*, 2005). This is observed in environmental conditions requiring similar performance abilities: distinct morphologies are then able to adapt to similar functional demands (Wainwright, 2005; Young *et al.*, 2007, 2010). This functional convergence could be explained by an increase in the selective pressures caused by fewer or different resources compared to previous layers, as the transition to L5 is towards a more arid environment (Stoetzel, 2009; El Hajraoui *et al.*, 2012).

In L4a, the morphological group of soft diet shrews is not present anymore. It must have disappeared during the previous arid period during which soft resources may have been scarce. It is known that the insect cuticle becomes harder under drier environments (Klocke & Schmitz, 2011). The cMP of the two remaining groups diverged distinctly. The supposed strong selection pressure(s) leading previously to the functional convergence in L5 must have eased. This is congruent with existing environmental inferences, as the environment in L4a is hypothesized to be very similar to conditions in L6 (Stoetzel, 2009; El Hajraoui *et al.*, 2012). In L3, the divergence between cMP of the two groups increases. We can hypothesize that those two shrew morphotypes were subject to functional divergence. Each group of shrews may have specialized in the acquisition of a different food resource. The group displaying high cMP specializing in hard, large objects, requiring mechanical potential with an important contribution from the temporalis, and the other group specializing on softer, smaller items, which requires less contribution of the temporalis. This divergence might be caused by competition occurring among shrews. Such a competition has been suggested between *C. russula* and other shrews species at EH2 at the exact same period (Cornette *et al.*, 2015c), and shrew dietary specialization might be a response to competition (Smith & Remington, 1996). In L2, a second diversity drop is observed with the disappearance of the group of hard diet specialists. As in L5, this event occurred following an arid period during which less diverse resources may have been available. Only the group of generalist shrews is continuously present up to present day.

Interestingly, extant shrews display a particularly weak cMP. This may be caused by the recent deterioration of climatic conditions linked to the increase of human pressure (Lewis & Maslin, 2015). Once again, it might be explained by a release of selective pressures on the temporalis resulting from a switch in diet (Santana *et al.*, 2010). Another explanation might be a selection towards weaker cMP. This is counter-intuitive, however, as selection for lower performance likely only occurs when the trait is energetically expensive to maintain or involved in trade-offs with other more relevant traits (Irschick *et al.*, 2008). The energy previously allocated to the mechanical potential of the temporalis might have been reallocated to another performance trait under stronger selection in the novel environment.

CONCLUSION

To conclude, results of the present study illustrate the relevance of functional traits to detect palaeoenvironmental transitions. Estimated bite forces showed variation in relation to palaeoenvironmental changes over the considered period (Late Pleistocene-Holocene), with a particular sensibility to transition between arid and humid environments. The complementary nature of morphological and functional indicators allowed to infer and discuss the possible evolutionary and ecological processes involved. Functional traits have a great potential for refining palaeoenvironmental and palaeoecological inferences. Moreover, they appear to be relevant indicators of palaeoenvironmental transitions and offer a range of opportunities to explore the impact of environmental changes on extinct organisms.

ACKNOWLEDGEMENTS

The authors would like to thank the Mission Archéologique El Harhoura-Témara, the Ministère des Affaires Etrangères et Européennes, France, the Ministère de la Culture, Morocco (directors R. Nespoulet and M.A. El Hajraoui), the Institut National des Sciences de l'Archéologie et du Patrimoine (INSAP), Rabat, Morocco, and the Institut Scientifique, Rabat, Morocco, for helping to provide modern and fossil shrew specimens. This research was funded by the Université Paris Descartes, the Ecole Doctorale FIRE-Programme Bettencourt. We also thank the two anonymous reviewers for constructive comments that helped to greatly improve the manuscript. The authors declare that they have no conflicts of interest.

REFERENCES

Adams DC. 2016. Evaluating modularity in morphometric data: challenges with the RV coefficient and a new test measure. *Methods in Ecology and Evolution* **7:** 565–572.

Adams DC, **Otárola-Castillo E. 2013.** geomorph: an R package for the collection and analysis of geometric morphometric shape data. *Methods in Ecology and Evolution* **4:** 393–399.

Alfaro ME, **Bolnick DI**, **Wainwright PC. 2005.** Evolutionary consequences of many-to-one mapping of jaw morphology to mechanics in labrid fishes. *The American Naturalist* **165:** E140–E154.

Alperin MI, **Cusminsky GC**, **Bernasconi E. 2011.** Benthic foraminiferal morphogroups on the Argentine continental shelf. *The Journal of Foraminiferal Research* **41:** 155–166.

Anderson RA, **McBrayer LD**, **Herrel A. 2008.** Bite force in vertebrates: opportunities and caveats for use of a nonpareil whole-animal performance measure. *Biological Journal of the Linnean Society* **93:** 709–720.

Arnold SJ. 1983. Morphology, performance and fitness. *American Zoologist* **23:** 347–361.

Badyaev AV, **Foresman KR. 2000.** Extreme environmental change and evolution: stress-induced morphological variation is strongly concordant with patterns of evolutionary divergence in shrew mandibles. *Proceedings. Biological Sciences* **267:** 371–377.

Badyaev AV, **Foresman KR. 2004.** Evolution of morphological integration. I. Functional units channel stress-induced variation in shrew mandibles. *The American Naturalist* **163:** 868–879.

Baylac M, **Frieß M. 2005.** Fourier descriptors, Procrustes superimposition, and data dimensionality: an example of cranial shape analysis in modern human populations. In: Slice DE, ed. *Modern morphometrics in physical anthropology.* New York: Kluwer Academic Publishers-Plenum Publishers, 145–165.

Ben Arous E, **Falguères C**, **Nespoulet R**, **El Hajraoui MA. 2020a.** Review of chronological data from the Rabat-Temara caves (Morocco): implications for understanding human occupation in north-west Africa during the Late Pleistocene. In: Leplongeon A, Goder-Goldberger M, Pleurdeau D, eds. *Not just a corridor. Human occupation of the Nile Valley and neighbouring regions between 75 000 and 15 000 years ago*, Paris, Muséum national d'Histoire naturelle (Natures en Sociétés; 3) 177–201.

Ben Arous E, **Falguères C**, **Tombret O**, **El Hajraoui MA**, & **Nespoulet R. 2020b.** Combined US-ESR dating of fossil teeth from El Harhoura 2 cave (Morocco): New data about the end of the MSA in Temara region. *Quaternary International* **556:** 88–95.

Bergmann PJ, **McElroy EJ. 2014.** Many-to-many mapping of phenotype to performance: an extension of the F-matrix for studying functional complexity. *Evolutionary Biology* **41:** 546–560.

Bookstein FL. 1996. Landmark methods for forms without landmarks: morphometrics of group differences in outline shape. *Medical Image Analysis* **1:** 225–243.

Boutin S, **Lane JE. 2014.** Climate change and mammals: evolutionary versus plastic responses. *Evolutionary Applications* **7:** 29–41.

Brassard C, **Merlin M**, **Guintard C**, **Monchâtre-Leroy E**, **Barrat J**, **Bausmayer N**, **Bausmayer S**, **Bausmayer A**, **Beyer M**, **Varlet A**, **Houssin C**, **Callou C**, **Cornette R**, **Herrel A. 2020a.** Bite force and its relation to jaw shape in domestic dogs. *Journal of Experimental Biology* **223:** jeb224352.

Brassard C, **Merlin M**, **Monchâtre-Leroy E**, **Guintard C**, **Barrat J**, **Callou C**, **Cornette R**, **Herrel A. 2020b.** How does masticatory muscle architecture covary with mandibular shape in domestic dogs? *Evolutionary Biology* **47:** 133–151.

Casanovas-Vilar I, **van Dam J. 2013.** Conservatism and adaptability during squirrel radiation: what is mandible shape telling us? *PLoS One* **8:** e61298.

Caumul R, **Polly D. 2005.** Phylogenetic and environmental components of morphological variation: skull, mandible and molar shape in marmots (*Marmota*, Rodentia). *Evolution* **59:** 2460–2472.

Chazeau C, **Marchal J**, **Hackert R**, **Perret M**, **Herrel A. 2013.** Proximate determinants of bite force capacity in the mouse lemur. *Journal of Zoology* **290:** 42–48.

Cheverud JM, **Routman EJ**, **Irschick DJ. 1997.** Pleiotropic effects of individual gene loci on mandibular morphology. *Evolution; International Journal of Organic Evolution* **51:** 2006–2016.

Christiansen P, **Wroe S. 2007.** Bite forces and evolutionary adaptations to feeding ecology in carnivores. *Ecology* **88:** 347–358.

Comay O, **Weissbrod L**, **Dayan T. 2019.** Predictive modelling in paleoenvironmental reconstruction: the micromammals of Manot Cave, Israel. *Journal of Human Evolution* In Press.

Cornette R, **Baylac M**, **Souter T**, **Herrel A. 2013.** Does shape co-variation between the skull and the mandible have functional consequences? A 3D approach for a 3D problem. *Journal of Anatomy* **223:** 329–336.

Cornette R, **Herrel A**, **Stoetzel E**, **Moulin S**, **Hutterer R**, **Denys C**, **Baylac M. 2015a.** Specific information levels in relation to fragmentation patterns of shrew mandibles: do fragments tell the same story? *Journal of Archaeological Science* **53:** 323–330.

Cornette R, **Stoetzel E**, **Baylac M**, **Moulin S**, **Hutterer R**, **Nespoulet R**, **El Hajraoui MA**, **Denys C**, **Herrel A. 2015c.** Shrews of the genus *Crocidura* from El Harhoura 2 (Témara, Morocco): the contribution of broken specimens to the understanding of Late Pleistocene–Holocene palaeoenvironments in North Africa. *Palaeogeography, Palaeoclimatology, Palaeoecology* **436:** 1–8.

Cornette R, **Tresset A**, **Houssin C**, **Pascal M**, **Herrel A. 2015b.** Does bite force provide a competitive advantage in shrews? The case of the greater white-toothed shrew. *Biological Journal of the Linnean Society* **114:** 795–807.

Dumont ER, **Herrel A**, **Medellin RA**, **Vargas-Contreras JA**, **Santana SE. 2009.** Built to bite: cranial design and function in the wrinkle-faced bat. *Journal of Zoology* **279:** 329–337.

El Hajraoui MA, **Nespoulet R**, **Debénath A**, **Dibble HL, eds. 2012.** La Préhistoire de la région de Rabat-Témara. Institut National des Sciences de l'Archéologie et du Patrimoine: *Villes et Sites Archéologiques du Maroc*. p. 300.

Erickson GM, **Kirk SDV**, **Su J**, **Levenston ME**, **Caler WE**, **Carter DR. 1996.** Bite-force estimation for *Tyrannosaurus rex* from tooth-marked bones. *Nature* **382:** 706–708.

Erwin DH. 2000. Macroevolution is more than repeated rounds of microevolution. *Evolution & Development* **2:** 78–84.

Escudé É, **Renvoisé É**, **Lhomme V**, **Montuire S. 2013.** Why all vole molars (Arvicolinae, Rodentia) are informative to be considered as proxy for Quaternary paleoenvironmental reconstructions. *Journal of Archaeological Science* **40:** 11–23.

Fernández-Jalvo Y, **Denys C**, **Andrews P**, **Williams T**, **Dauphin Y**, **Humphrey L. 1998.** Taphonomy and palaeoecology of Olduvai Bed-I (Pleistocence, Tanzania). *Journal of Human Evolution* **34:** 137–172.

Freeman PW. 1979. Specialized insectivory: beetle-eating and moth-eating molossid bats. *Journal of Mammalogy* **60:** 467–479.

Freeman PW, **Lemen CA. 2008.** A simple morphological predictor of bite force in rodents. *Journal of Zoology* **275:** 418–422.

Furió M, **Agustí J**, **Mouskhelishvili A**, **Sanisidro Ó**, **Santos-Cubedo A. 2010.** The paleobiology of the extinct venomous shrew *Beremendia* (Soricidae, Insectivora, Mammalia) in relation to the geology and paleoenvironment of Dmanisi (Early Pleistocene, Georgia). *Journal of Vertebrate Paleontology* **30:** 928–942.

Garland T, **Losos JB. 1994.** Ecological morphology of locomotor performance in squamate reptiles. In: Wainwright PC, Reilly SM, eds. *Ecological morphology: integrative organismal biology*. Chicago: University of Chicago Press, 240–302.

Ginot S, **Herrel A**, **Claude J**, **Hautier L. 2018.** Skull size and biomechanics are good estimators of *in vivo* bite force in murid rodents: *in vivo* bite force estimation in murid rodents. *The Anatomical Record* **301:** 256–266.

Ginot S, **Herrel A**, **Claude J**, **Hautier L. 2019.** Morphometric models for estimating bite force in *Mus* and *Rattus*: mandible shape and size perform better than lever-arm ratios. *The Journal of Experimental Biology* **222:** jeb204867.

Goswami A, **Smaers JB**, **Soligo C**, **Polly PD. 2014.** The macroevolutionary consequences of phenotypic integration: from development to deep time. *Philosophical Transactions of the Royal Society of London. Series B, Biological Sciences* **369:** 20130254.

Gunz P, **Mitteroecker P**, **Bookstein FL. 2005.** Semilandmarks in three dimensions. In: Slice DE, ed. *Modern morphometrics in physical anthropology.* New York: Kluwer Academic Publishers-Plenum Publishers, 73–98.

Hautmann M. 2020. What is macroevolution? *Palaeontology* **63:** 1–11.

Herrel A, **De Smet A**, **Aguirre LF**, **Aerts P. 2008.** Morphological and mechanical determinants of bite force in bats: do muscles matter? *The Journal of Experimental Biology* **211:** 86–91.

Herrel A, **O'Reilly JC**, **Richmond AM. 2002.** Evolution of bite performance in turtles. *Journal of Evolutionary Biology* **15:** 1083–1094.

Holzman R, **Collar DC**, **Mehta RS**, **Wainwright PC. 2011.** Functional complexity can mitigate performance trade-offs. *The American Naturalist* **177:** 1–15.

Huber DR, **Eason TG**, **Hueter RE**, **Motta PJ. 2005.** Analysis of the bite force and mechanical design of the feeding mechanism of the durophagous horn shark *Heterodontus francisci*. *The Journal of Experimental Biology* **208:** 3553–3571.

Irschick DJ, **Meyers JJ**, **Husak JF**, **Galliard JFL. 2008.** How does selection operate on whole-organism functional performance capacities? A review and synthesis. *Evolutionary Ecology Research* **10:** 177–196.

Jacobs Z, **Roberts RG. 2012**. Chapitre III. Datations par OSL avec la technique du grain unique. In: El Hajraoui MA, Nespoulet R, Debénath A, Dibble HL, eds. *La Préhistoire de la région de Rabat-Témara*. Institut National des Sciences de l'Archéologie et du Patrimoine: Villes et Sites Archéologiques du Maroc, p. 300.

Jacobs Z, **Roberts RG**, **Nespoulet R**, **El Hajraoui MA**, **Debénath A. 2012.** Single-grain OSL chronologies for Middle Palaeolithic deposits at El Mnasra and El Harhoura 2, Morocco: implications for Late Pleistocene human-environment interactions along the Atlantic coast of northwest Africa. *Journal of Human Evolution* **62:** 377–394.

Janati-Idrissi N, **Falgueres C**, **Nespoulet R**, **El Hajraoui MA**, **Debénath A**, **Bejjit L**, **Bahain JJ**, **Michel P**, **Garcia T**, **Boudad L**, **El Hammouti K**, **Oujaa A. 2012.** Datation par ESR-U/th combinées de dents fossiles des grottes d'El Mnasra et d'El Harhoura 2, région de Rabat-Temara. Implications chronologiques sur le peuplement du Maroc atlantique au Pléistocène supérieur et son. *Quaternaire*: **23:** 25–35.

Kaufman L, **Rousseeuw PJ. 1990.** *Finding groups in data: an introduction to cluster analysis*. *Wiley Series in Probability and Mathematical Statistics. Applied Probability and Statistics*. New York: Wiley.

Kerr E, **Cornette R**, **Rodrigues HG**, **Renaud S**, **Chevret P**, **Tresset A**, **Herrel A. 2017.** Can functional traits help explain the coexistence of two species of *Apodemus*? *Biological Journal of the Linnean Society*: **122:** 883–896.

Khare N, **Nigam R**, **Mayenkar DN**, **Saraswat R. 2017.** Cluster analysis of benthic foraminiferal morpho-groups from the western margin of India reflects its depth preference. *Continental Shelf Research* **151:** 72–83.

Klingenberg CP. 2004. Integration and modularity of quantitative trait locus effects on geometric shape in the mouse mandible. *Genetics* **166:** 1909–1921.

Klingenberg CP. 2008. Morphological integration and developmental modularity. *Annual Review of Ecology, Evolution, and Systematics* **39:** 115–132.

Klingenberg CP. 2016. Size, shape, and form: concepts of allometry in geometric morphometrics. *Development Genes and Evolution* **226:** 113–137.

Klingenberg CP, **Marugán-Lobón J. 2013.** Evolutionary covariation in geometric morphometric data: analyzing integration, modularity, and allometry in a phylogenetic context. *Systematic Biology* **62:** 591–610.

Klingenberg CP, **Mebus K**, **Auffray JC. 2003.** Developmental integration in a complex morphological structure: how distinct are the modules in the mouse mandible? *Evolution & Development* **5:** 522–531.

Klocke D, **Schmitz H. 2011.** Water as a major modulator of the mechanical properties of insect cuticle. *Acta Biomaterialia* **7:** 2935–2942.

Lande R. 2009. Adaptation to an extraordinary environment by evolution of phenotypic plasticity and genetic assimilation. *Journal of Evolutionary Biology* **22:** 1435–1446.

Langerhans RB. 2009. Trade-off between steady and unsteady swimming underlies predator-driven divergence

in *Gambusia affinis*. *Journal of Evolutionary Biology* **22:** 1057–1075.

Lappin AK, **Wilcox SC**, **Moriarty DJ**, **Stoeppler SAR**, **Evans SE**, **Jones MEH. 2017.** Bite force in the horned frog (*Ceratophrys cranwelli*) with implications for extinct giant frogs. *Scientific Reports* **7:** 11963.

Lewis SL, **Maslin MA. 2015**. Defining the Anthropocene. *Nature* **519:** 171–180.

López-García JM, **Cuenca-Bescós G**, **Galindo-Pellicena MÁ**, **Luzi E**, **Berto C**, **Lebreton L**, **Desclaux E. 2021.** Rodents as indicators of the climatic conditions during the Middle Pleistocene in the southwestern Mediterranean region: implications for the environment in which hominins lived. *Journal of Human Evolution* **150:** 102911.

Losos JB. 1992. The evolution of convergent structure in Caribbean *Anolis* communities. *Systematic Biology* **41:** 18.

Maestri R, **Patterson BD**, **Fornel R**, **Monteiro LR**, **de Freitas TR. 2016.** Diet, bite force and skull morphology in the generalist rodent morphotype. *Journal of Evolutionary Biology* **29:** 2191–2204.

Manhães IA, **Nogueira MR**, **Monteiro LR. 2017.** Bite force and evolutionary studies in phyllostomid bats: a meta-analysis and validation. *Journal of Zoology* **302:** 288–297.

McGuire JL. 2010. Geometric morphometrics of vole (*Microtus californicus*) dentition as a new paleoclimate proxy: shape change along geographic and climatic clines. *Quaternary International* **212:** 198–205.

Mevik BH, **Wehrens R. 2007.** The pls package: principal component and partial least squares regression in R. *Journal of Statistical Software* **18:** 1–23.

Mezey JG, **Cheverud JM**, **Wagner GP. 2000.** Is the genotype-phenotype map modular? A statistical approach using mouse quantitative trait loci data. *Genetics Society of America* **156:** 305–311.

Monteiro LR, **Nogueira MR. 2011.** Evolutionary patterns and processes in the radiation of phyllostomid bats. *BMC Evolutionary Biology* **11:** 137.

Nancy AN. 1982. *The big cats: the paintings of Guy Coheleach.* New York: Abradale/Abrams.

Nespoulet R, **El Hajraoui MA**, **Amani F**, **Ben Ncer A**, **Debénath A**, **El Idrissi A**, **Lacombe JP**, **Michel P**, **Oujaa A**, **Stoetzel E. 2008.** Palaeolithic and Neolithic occupations in the Témara Region (Rabat, Morocco): recent data on hominin contexts and behavior. *African Archaeological Review* **25:** 21–39.

Nogueira MR, **Peracchi AL**, **Monteiro LR. 2009.** Morphological correlates of bite force and diet in the skull and mandible of phyllostomid bats. *Functional Ecology* **23:** 715–723.

R Core Team. 2020. *R: A language and environment for statistical computing*. Vienna, Austria: R Foundation for Statistical Computing. Available at: http://www.R-project.org/

Read CF, **Duncan DH**, **Vesk PA**, **Elith J. 2014.** Biocrust morphogroups provide an effective and rapid assessment tool for drylands. *Journal of Applied Ecology* **51:** 1740–1749.

Rinderknecht A, **Jones WW**, **Araújo N**, **Grinspan G**, **Blanco RE. 2019.** Bite force and body mass of the fossil rodent *Telicomys giganteus* (Caviomorpha, Dinomyidae). *Historical Biology* **31:** 644–652.

Rohlf FJ, **Slice D. 1990.** Extensions of the Procrustes method for the optimal superimposition of landmarks. *Systematic Zoology* **39:** 40.

Royer A, **Garcia Yelo BA**, **Laffont R**, **Hernandez Fernandez M. 2020.** New bioclimatic models for the Quaternary Palaearctic based on insectivore and rodent communities. *Palaeogeography, Palaeoclimatology, Palaeoecology* **560:** 18.

Santana SE, **Dumont ER**, **Davis JL. 2010.** Mechanics of bite force production and its relationship to diet in bats. *Functional Ecology* **24:** 776–784.

Schwenk K. 2000. *Form, function, and evolution in tetrapod vertebrates.* Academic Press.

Smith HR, **Remington CL. 1996.** Food specificity in interspecies competition. *BioScience* **46:** 436–447.

Souquet L, **Chevret P**, **Ganem G**, **Auffray JC**, **Ledevin R**, **Agret S**, **Hautier L**, **Renaud S. 2019.** Back to the wild: does feralization affect the mandible of non-commensal house mice (*Mus musculus domesticus*)? *Biological Journal of the Linnean Society* **126:** 471–486.

Stayton CT. 2006. Testing hypotheses of convergence with multivariate data: morphological and functional convergence among herbivorous lizards. *Evolution; International Journal of Organic Evolution* **60:** 824–841.

Stoetzel E. 2009. Les microvertébrés du site d'occupation humaine d'El Harhoura 2 (Pleistocene supérieur–Holocène, Maroc): systématique, évolution, taphonomie et paléoécologie. Muséum national d'Histoire naturelle, doctoral dissertation.

Stoetzel E. 2017. Adaptations and dispersals of anatomically modern humans in the changing environments of North Africa: the contribution of microvertebrates. *African Archaeological Review* **34:** 453–468.

Stoetzel E, **Bailon S**, **Nespoulet R**, **El Hajraoui MA**, **Denys C. 2010.** Pleistocene and Holocene small vertebrates of El Harhoura 2 cave (Rabat-Témara, Morocco): an annotated preliminary taxonomic list. *Historical Biology* **22:** 303–319.

Stoetzel E, **Bougariane B**, **Campmas E**, **Ouchaou B**, **Michel P. 2012a.** Chapitre V. Faunes et paléoenvironnements. In: *La Préhistoire de la région de Rabat-Témara*. El Hajraoui MA, Nespoulet R, Debénath A & Dibble HL (eds). Institut National des Sciences de l'Archéologie et du Patrimoine: Villes et Sites Archéologiques du Maroc. 300 p.

Stoetzel E, **Campmas E**, **Michel P**, **Bougariane B**, **Ouchaou B**, **Amani F**, **El Hajraoui MA**, **Nespoulet R. 2014.** Context of modern human occupations in North Africa: contribution of the Témara caves data. *Quaternary International* **320:** 143–161.

Stoetzel E, **Cornette R**, **Lalis A**, **Nicolas V**, **Cucchi T**, **Denys C. 2017.** Systematics and evolution of the *Meriones shawii/grandis* complex (Rodentia, Gerbillinae) during the Late Quaternary in northwestern Africa: exploring the role of environmental and anthropogenic changes. *Quaternary Science Reviews* **164:** 199–216.

Stoetzel E, **Denys C**, **Bailon S**, **El Hajraoui MA**, **Nespoulet R. 2012b.** Taphonomic analysis of amphibian

and squamate remains from El Harhoura 2 (Rabat-Témara, Morocco): contributions to palaeoecological and archaeological interpretations. *International Journal of Osteoarchaeology* **22:** 616–635.

Stoetzel E, **Denys C**, **Michaux J**, **Renaud S. 2013.** *Mus* in Morocco: a Quaternary sequence of intraspecific evolution. *Biological Journal of the Linnean Society* **109:** 599–621.

Stoetzel E, **Marion L**, **Nespoulet R**, **El Hajraoui MA**, **Denys C. 2011.** Taphonomy and palaeoecology of the late Pleistocene to middle Holocene small mammal succession of El Harhoura 2 cave (Rabat-Témara, Morocco). *Journal of Human Evolution* **60:** 1–33.

Therrien F. 2005. Feeding behaviour and bite force of sabretoothed predators. *Zoological Journal of the Linnean Society* **145:** 393–426.

Valenzuela S, **Poitevin F**, **Cornette R**, **Bournery A**, **Nadal J**, **Vigne JD. 2009.** Evolving ecosystems: ecological data from an Iron Age small mammal accumulation at Alorda Park (Catalonia, Spain). *Journal of Archaeological Science* **36:** 1248–1255.

Van Damme R, **Vanhooydonck B**, **Aerts P**, **De Vree F. 2003.** Evolution of lizard locomotion: context and constraint. In: Bels VC, Gasc JP, Casinos A, eds. *Vertebrate biomechanics and evolution*. Oxford, England: BIOS Scientific Publishers Ltd, 267–282.

Vanhooydonck B, **Boistel R**, **Fernandez V**, **Herrel A. 2011.** Push and bite: trade-offs between burrowing and biting in a burrowing skink (*Acontias percivali*). *Biological Journal of the Linnean Society* **102:** 91–99.

Venables WN, **Ripley BD. 2002.** Modern applied statistics with S. Springer. 504 p.

Verde Arregoitia LD, **Fisher DO**, **Schweizer M. 2017**. Morphology captures diet and locomotor types in rodents. *Royal Society Open Science* **4:** 160957.

Wainwright PC. 1994. Functional morphology as a tool in ecological research. In: *Wainwright PC, Reilly SM, eds. Ecological morphology*, Chicago: The University of Chicago Press, 42–59.

Wainwright PC, **Alfaro ME**, **Bolnick DI**, **Hulsey CD. 2005.** Many-to-one mapping of form to function: a general principle in organismal design? *Integrative and Comparative Biology* **45:** 256–262.

Walker JA. 2007. A general model of functional constraints on phenotypic evolution. *The American Naturalist* **170:** 681–689.

Walker JA. 2010. An integrative model of evolutionary covariance: a symposium on body shape in fishes. *Integrative and Comparative Biology* **50:** 1051–1056.

Wang X, **Qiu W**, **Zamar RH. 2007.** CLUES: a non-parametric clustering method based on local shrinking. *Computational Statistics & Data Analysis* **52:** 286–298.

Wroe S, **McHenry C**, **Thomason J. 2005.** Bite club: comparative bite force in big biting mammals and the prediction of predatory behaviour in fossil taxa. *Proceedings. Biological Sciences* **272:** 619–625.

Young RL, **Badyaev AV. 2006.** Evolutionary persistence of phenotypic integration: influence of developmental and functional relationships on complex trait evolution. *Evolution; International Journal of Organic Evolution* **60:** 1291–1299.

Young RL, **Haselkorn TS**, **Badyaev AV. 2007.** Functional equivalence of morphologies enables morphological and ecological diversity. *Evolution; International Journal of Organic Evolution* **61:** 2480–2492.

Young RL, **Sweeney MJ**, **Badyaev AV. 2010.** Morphological diversity and ecological similarity: versatility of muscular and skeletal morphologies enables ecological convergence in shrews. *Functional Ecology* **24:** 556–565.

Zelditch M, ed. 2004. *Geometric morphometrics for biologists: a primer*. Amsterdam; Boston: Elsevier Academic Press.

SUPPORTING INFORMATION

Additional Supporting Information may be found in the online version of this article at the publisher's web-site:

Table S1. Couples of *a* and *b* tested on the simulated data set of bite forces and cMPs to assess the reliability of cMP as an estimator of bite force.

Figure S1. Global changes in Csize (A) and Csize per morphological group (B) of the shrews of EH2, from L8 until present day (Act). Environmental conditions (Stoetzel, 2009; El Hajraoui *et al.*, 2012) are indicated by background colours. Standard deviation is indicated for each point. B, black is the first morphological group; red is the second morphological group; blue is the third morphological group.

Figure S2. Global changes in the moment arm of the temporalis (A on Fig. 3) (A) and lever arm of the temporalis per morphological group (B) of the shrews of EH2, from L8 until present day (Act). Environmental conditions (Stoetzel, 2009; El Hajraoui *et al.*, 2012) are indicated by background colours. Standard deviation is indicated for each point. B, black is the first morphological group; red is the second morphological group; blue is the third morphological group.